Isotope exchange reactions involving HCO+ with CO: A theoretical approach

M. Mladenović, E. Roueff

Astronomy & Astrophysics

Isotope exchange reactions involving HCO⁺ with CO: A theoretical approach

M. Mladenović[1] and E. Roueff[2]

[1] Université Paris-Est, Laboratoire Modélisation et Simulation Multi Echelle, MSME UMR 8208 CNRS, 5 bd Descartes, 77454 Marne-la-Vallée, France
e-mail: Mirjana.Mladenovic@u-pem.fr
[2] LERMA, Observatoire de Paris, PSL Research University, CNRS, Sorbonne Universités, UPMC Univ. Paris 06, 92190 Meudon, France
e-mail: evelyne.roueff@obspm.fr

ABSTRACT

Aims. We aim to investigate fractionation reactions involved in the $^{12}C/^{13}C$, $^{16}O/^{18}O$, and ^{17}O balance.
Methods. Full-dimensional rovibrational calculations were used to compute numerically exact rovibrational energies and thermal equilibrium conditions to derive the reaction rate coefficients. A nonlinear least-squares method was employed to represent the rate coefficients by analytic functions.
Results. New exothermicities are derived for 30 isotopic exchange reactions of HCO⁺ with CO. For each of the reactions, we provide the analytic three-parameter Arrhenius-Kooij formula for both the forward reaction and backward reaction rate coefficients, that can further be used in astrochemical kinetic models. Rotational constants derived here for the ^{17}O containing forms of HCO⁺ may assist detection of these cations in outer space.

Key words. ISM: general – ISM: molecules – ISM: abundances

1. Introduction

The ^{18}O and ^{17}O isotopic variants of CO are routinely detected in interstellar galactic and extragalactic environments and are used to determine the evolution trend of the corresponding $^{18}O/^{17}O$ ratio through the galactic disk. However, HC$^{17}O^+$ has, to our knowledge, only been detected in two sources, SgB2 by Guélin et al. (1982) and in the molecular peak of the L1544 prestellar core by Dore et al. (2001a), who also refined the spectroscopic constants and the hyperfine coupling constants as the ^{17}O nucleus has a spin of 5/2. With the advent of sensitive receivers and large collecting areas available in modern observational facilities, such as ALMA and NOEMA, there is no doubt that more observations of these molecular ions will become available. However, the chemical reactions which may occur and possibly enhance the abundance of this rare molecular ion through isotopic exchange reactions, such as those occurring for HC$^{18}O^+$ (Mladenović & Roueff 2014), have not yet been reported. The purpose of the present study is to derive accurate values of the exothermicities involved in isotopic exchange reactions and to propose the corresponding reaction rate coefficients which can further be used in astrochemical models.

The fractionation of stable isotopes can be ascribed to a combination of the mass dependent thermodynamic (equilibrium) partition functions, the mass dependent diffusion coefficients, and the mass dependent reaction rate coefficients. This is in accordance with quantum mechanics, which predicts that mass affects the strength of chemical bonds and the vibrational, rotational, and translational motions, so that temperature dependent isotope fractionations may arise from quantum mechanical effects on rovibrational motion. For a given

vibrational state, the vibrational energy is lower for a bond involving a heavier isotope. The extent of isotopic fractionation varies inversely with temperature and is large at low temperatures.

Smith & Adams (1980) measured the forward k_f and reverse k_r rate coefficients for three isotopic variants of the reaction HCO⁺ with CO at 80, 200, 300, and 510 K using a selected ion flow tube (SIFT) technique. Langer et al. (1984) extrapolated the experimental values of Smith & Adams (1980) to temperatures below 80 K toward the limit of the average dipole orientation model of ion-polar molecule capture collisions (Su & Bowers 1975), producing the total rate coefficients $k_T = k_f + k_r$ for nine temperatures over the range 5–300 K. Langer et al. employed a common reduced mass for three isotopic variants of HCO⁺+CO studied by Smith & Adams (1980). The values for k_T were used in combination with theoretical spectroscopic parameters calculated for the isotopic variants of HCO⁺ by Henning et al. (1977) in order to model cosmochemical carbon and oxygen isotope fractionations. From the total mass-independent rate coefficients k_T and the theoretical zero point energy differences ΔE, Langer et al. (1984) estimated the rate coefficients k_f and k_r for six reactions HCO⁺+CO involving isotopologues containing ^{12}C, ^{13}C, ^{16}O, and ^{18}O.

Recently, we have investigated in some detail the isotope fractionation reactions of HCO⁺/HOC⁺ with CO and of N₂H⁺ with N₂ (Mladenović & Roueff 2014), hereafter called Paper I. In Paper I, we employed the global three-dimensional potential energy surfaces developed by Mladenović & Schmatz (1998) for the isomerizing system HCO⁺/HOC⁺ and by Schmatz & Mladenović (1997) for the isoelectronic species N₂H⁺ in combination with a numerically exact method

for the rovibrational calculations (Mladenović & Bačić 1990; Mladenović 2002). For the reaction HCO$^+$+CO, we pointed out inaccuracies of previous exothermicity values, which have been commonly used in chemical networks. The new exothermicities are found to affect significantly the rate coefficients derived at 10 K, corresponding to the temperature of dark interstellar cloud environments.

The isotopes H, D, ^{12}C, ^{13}C, ^{16}O, and ^{18}O were considered in our previous work (Mladenović & Roueff 2014), resulting in six reactions HCO$^+$+CO involving hydrogen and six reactions DCO$^+$+CO involving deuterium. In the present work, we extend our analysis with the stable isotope ^{17}O. The possible isotopic variants of HCO$^+$ and CO are connected by 15 reactions for the hydrogenic forms and 15 reactions for the deuterated counterparts. All 30 were studied here. Nominal abundances of oxygen isotopes ^{16}O, ^{17}O, and ^{18}O are 99.76, 0.04, and 0.20%, respectively (Mills et al. 1993).

Our theoretical approach is described in Sect. 2. In Sect. 3, we report the energies involved in all possible exchange reactions between CO and HCO$^+$ (HOC$^+$) isotopologues and their deuterium variants, as well as the rate coefficients for the reaction of HCO$^+$ with CO in the 5–300 K temperature window. We summarize our finding in Sect. 4.

2. Methods

Isotopic exchange reactions can occur according to different types as discussed in Roueff et al. (2015). However, the equilibrium constant K_e, which provides the ratio of the forward reaction rate coefficient k_f and the backward (reverse) reaction rate coefficient k_r, is uniquely defined under thermal equilibrium conditions.

We considered the exchange between an heavy (H) and light (L) isotope in the reaction

$$AL + BH \underset{k_r}{\overset{k_f}{\rightleftharpoons}} AH + BL. \tag{1}$$

Under thermal equilibrium conditions, the equilibrium constant K_e is given by

$$K_e = \frac{k_f}{k_r} = F_q \, e^{\Delta E/k_B T}, \tag{2}$$

using

$$F_q = f_m^{3/2} \frac{Q_{int}(AH) \, Q_{int}(BL)}{Q_{int}(AL) \, Q_{int}(BH)}, \tag{3}$$

and

$$f_m = \frac{m(AH) \, m(BL)}{m(AL) \, m(BH)}, \tag{4}$$

where $m(X)$ stands for the mass of the species X. In Eq. (2), ΔE is the zero point energy difference between the reactants and the products,

$$\Delta E = E_0(AL) + E_0(BH) - E_0(AH) - E_0(BL). \tag{5}$$

To express ΔE in Kelvin, we used $\Delta E/k_B$, where k_B is the Boltzmann constant. The zero point energy $E_0(X)$ for the species X is measured on an absolute energy scale. In practical applications, $E_0(X)$ is given relative to the respective potential energy minimum. The electronic states are not changed in the course of the reaction of Eq. (1), so that the ratio of the electronic partition functions is unity in Eq. (3). The term f_m arises from

the translational contribution. For the internal partition function Q_{int}, we used

$$Q_{int} = g \sum_J \sum_i (2J + 1) \, e^{-\varepsilon_i^J/k_B T}, \tag{6}$$

where $\varepsilon_i^J = E_i^J - E_0^0$ denotes the rovibrational energy for a total angular momentum J. The factor $2J + 1$ accounts for the degeneracy with respect to the space-fixed reference frame and g for the nuclear spin degeneracy. Additional care is required for the nuclear spin degeneracy factor when different spin states (e.g., ortho or para) are involved either in the reactants or in the products, as discussed in Terzieva & Herbst (2000). The rovibrational energies ε_i^J are measured relative to the corresponding zero point energy E_0^0.

For all the species involved in the reaction considered, the rovibrational energies ε_i^J are computed by theoretical means, considering explicitly the quantum mechanical effects due to vibrational anharmonicities and rovibrational couplings. The energies ε_i^J are used to evaluate the partition functions Q_{int} of Eq. (6) for a given temperature and then to compute the equilibrium constant K_e of Eq. (2). This approach has been pursued also in Paper I.

If the exchange proceeds through the formation of an adduct which can dissociate both backwards and forwards, we can define a total rate coefficient k_T, which is often expressed as the capture rate constant,

$$k_T = k_f + k_r. \tag{7}$$

We then readily have

$$k_f = k_T \frac{K_e}{K_e + 1} \quad \text{and} \quad k_r = k_T \frac{1}{K_e + 1}. \tag{8}$$

Such a mechanism takes place for the isotopic exchange reaction of ^{13}C$^+$ with CO and isotopologues as well as for proton transfer reactions of the type

$$A + HB^+ \underset{k_r}{\overset{k_f}{\rightleftharpoons}} HA^+ + B, \tag{9}$$

where A and B are isotopologues of CO.

At low temperatures, the dominant term in the expression of Eq. (2) for the equilibrium constant K_e is the exponential term. Approximating $F_q \approx 1$, so that $K_e \approx e^{\Delta E/k_B T}$, it follows that

$$k_f \approx k_T \frac{1}{1 + e^{-\Delta E/k_B T}} \quad \text{and} \quad k_r \approx k_T \frac{e^{-\Delta E/k_B T}}{1 + e^{-\Delta E/k_B T}}. \tag{10}$$

The partition function factor F_q of Eq. (3) provides thus a quantitative estimate of the goodness of the approximation of Eq. (10), which is often employed in kinetic models at low temperatures.

3. Results and discussion

All the isotopic variants of ^{12}C, ^{13}C, ^{16}O, ^{17}O, and ^{18}O for CO, HCO$^+$/HOC$^+$, and DCO$^+$/DOC$^+$ are considered in this work. Using the global three-dimensional potential energy surface of Mladenović & Schmatz (1998) for the isomerizing system HCO$^+$/HOC$^+$, we calculate the rovibrational level energies for six isotopologues of HCO$^+$ and six isotopologues of DCO$^+$, as well as for HOC$^+$ and DOC$^+$. For isotopologues of CO, we employ the CCSD(T)/cc-pVQZ potential energy curve, developed previously (Mladenović & Roueff 2014). From these results, the zero point energy differences are readily determined for

the proton transfer reactions of Eq. (9) involving HCO$^+$ with CO and HOC$^+$ with CO. The equilibrium constants K_e as a function of temperature are evaluated according to Eq. (2) for the isotope exchange reactions HCO$^+$+CO, which have already been studied experimentally (Smith & Adams 1980).

The spectroscopic properties for the isotopologues of HCO$^+$ are summarized in Table A.1. The mode labels ν_1, ν_2, ν_3 refer respectively to the higher-frequency (CH) stretching vibration, the bending vibration, and the lower-frequency stretching (CO) vibration, whereby the bending vibration is doubly degenerate. By fitting the calculated ground state vibrational energies obtained for $0 \le J \le 15$ to the standard polynomial expression,

$$E_0(J) = B_0 J(J + 1) - D_0 [J(J + 1)]^2, \qquad (11)$$

we have derived the effective rotational constant B_0 and the quartic centrifugal distortion constant D_0 for the ground vibrational state. The ground state vibrational correction ΔB_0 to the equilibrium rotational constant B_e is given by

$$\Delta B_0 = B_e - B_0 = \tfrac{1}{2} (\alpha_1 + 2\alpha_2 + \alpha_3), \qquad (12)$$

where α_i is a vibration-rotation interaction constant for the ith vibration (Herzberg 1991). In this expression, we substitute our B_e values with the best estimate B_e^{est} of the equilibrium rotational constant, computed employing the best estimate of the equilibrium geometry $r_e(\text{HC}) = 1.09197\,\text{Å}$ and $r_e(\text{CO}) = 1.10546\,\text{Å}$ due to Puzzarini et al. (1996). This approach yields our best estimate B_0^{est} of the rotational constant for the ground vibrational state as $B_0^{\text{est}} = B_e^{\text{est}} - \Delta B_0$. As seen in Table A.1, all of the theoretical values for B_0^{est} agree with the available experimental B_0 values within 11 MHz. Similar accuracy can also be expected for other HCO$^+$ isotopologues that are not yet experimentally detected. For the fundamental vibrational transitions, our theoretical results agree within 5 cm^{-1} with the experimental findings. In the case of the quartic centrifugal distortion constants D_0, the agreement is within 4.5 kHz.

Direct proton transfer via the collinear approach from the carbon or oxygen side of CO to HCO$^+$/HOC$^+$ was studied in Paper 1 using the CCSD(T)/aug-cc-pVTZ electronic structure method. In all the cases analyzed there, the reaction was found to proceed through a stable intermediate proton-bound complex A-H-B$^+$ (see Eq. (9)), such that the reaction is barrierless in this description. In the case of the reaction involving HOC$^+$, it appears that the CO-catalyzed isomerisation is a more likely event than the proton transfer reaction, as seen in Fig. 2a of Paper 1.

3.1. Zero point energies

The ground state vibrational energies calculated in this work for isotopic variants of CO, HCO$^+$, and HOC$^+$ are collected in Table A.2. They are given relative to the corresponding potential energy minimum. On the potential energy surface for HCO$^+$/HOC$^+$, the global potential energy minimum is at -1.86 cm^{-1}. In assembling Table A.2, we noticed that Table 1 of Paper I did not incorporate the energy shift of 1.86 cm^{-1} for the zero point energies of D^{12}C^{16}O$^+$, D^{12}C^{18}O$^+$, D^{13}C^{16}O$^+$, and D^{13}C^{18}O$^+$. Accordingly, we list the zero point energies for all of the isotopologues of CO, HCO$^+$, and HOC$^+$ in Table A.2 of this work. We note that the other results of Paper I are not affected by this misprint.

The zero point energies are graphically displayed in Fig. 1 for the isotopic ^{12}C, ^{13}C, ^{16}O, ^{17}O, and ^{18}O variants of CO and HCO$^+$. The largest difference ΔE_{max} seen there is between the zero point energies for the lightest and heaviest forms, yielding
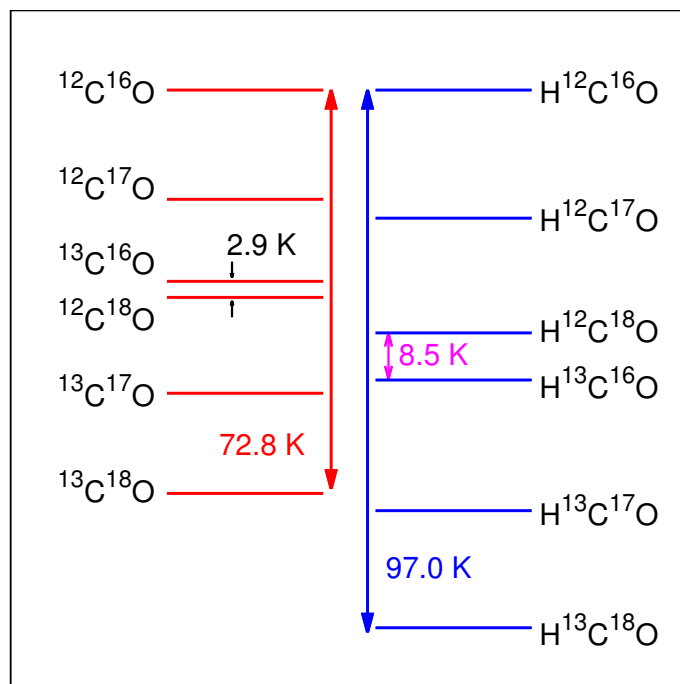

Fig. 1. Relative positions of the ground state vibrational energies of six isotopologues of CO and HCO$^+$.

$\Delta E_{\text{max}} = 72.8$ K for carbon monoxide and $\Delta E_{\text{max}} = 97.0$ K for the formyl cation. The species containing ^{17}O possess zero point energies lying between the zero point energies of the ^{18}O and ^{16}O forms in Fig. 1 and Table A.2.

3.2. Reactions of HCO$^+$ and HOC$^+$ with CO

The zero point energy differences for the proton transfer reactions CO+HCO$^+$/HOC$^+$ are presented in Table A.3. In accordance with the notation of Paper I, the reactions involving the formyl cation HCO$^+$ are labeled with F and the reactions involving the isoformyl cation HOC$^+$ with I. The deuterium variant of the reaction Fn is denoted by Fn(D), where $n = 1$–15, and similar for the other cases. The reactions F1-F6 involving the isotopes ^{16}O and ^{18}O were studied in some detail in Paper I. Inclusion of the isotope ^{17}O leads to nine additional reactions, which are denoted by F7-F15 and similar for the other variants. A complete list of possible reactions for the isotopes H, D, ^{12}C, ^{13}C, ^{16}O, ^{17}O, and ^{18}O is given in Table A.3. The exothermicities for the reactions F1-F6, F1(D)-F6(D), I1-I6, and I1(D)-I6(D) were already shown in Table 2 of Paper I. The proton transfer reactions I1 and I1(D) involving HOC$^+$ were also considered by Lohr (1998).

The largest ΔE in Table A.3 is associated with the reactions F5 and F5(D) in the case of HCO$^+$ and with the reactions I6 and I6(D) in the case of HOC$^+$. From Table A.3, we easily deduce that ^{13}C is preferentially placed in H/DCO$^+$ and a heavier O in H/DOC$^+$. The reactions involving the same isotope of C in HCO$^+$ and CO possess smaller exothermicities than the reactions involving different C isotopes, as seen by comparing for example, reaction F3 ($\Delta E = 6.4$ K) with reaction F5 ($\Delta E = 24.2$ K), which involve ^{18}O. The corresponding ^{17}O counterparts have somewhat smaller ΔE values, for example reaction F7 of $\Delta E = 3.4$ K versus reaction F11 of $\Delta E = 21.2$ K. In all cases, reactions involving deuterium possess slightly higher exothermicities, for example, ΔE for reactions F15 and F15(D)

are 20.8 K and 25.3 K, respectively. The reactions with the iso-formyl isomers have lower exothermicities than the reactions with the formyl forms. In several cases, the reactions $HOC^+ + CO$ proceed in the direction opposite to the direction of the corresponding $HCO^+ + CO$ reaction in accordance with the fact that the isotopic substitution of the central atom is thermodynamically favored. Table A.3 clearly exemplifies this effect.

The partition function factors F_q, the isotope exchange equilibrium constants K_e, and the rate coefficients (k_f, k_r) for several temperatures between 5 and 300 K are given in Table A.4 for reactions F7-F15 and F7(D)-F15(D). This table complements Table 5 of Paper I, which provides analogous information for reactions F1-F6 and F1(D)-F6(D). The values of K_e are obtained using Eq. (2) by direct evaluation of the internal partition functions Q_{int} from the computed rovibrational energies. The forward reaction k_f and backward reaction k_r rate coefficients are calculated according to Eq. (8) using our ΔE values of Table A.2 in combination with the total temperature dependent rate coefficients k_T given by Langer et al. (1984).

In Eq. (2), F_q is a mass and temperature dependent factor, defined by Eq. (3). Its temperature dependence is due to the temperature dependence of Q_{int}. The mass dependence of F_q comes from the translational contribution f_m. In addition, the mass affects the effective rotational constants for a given vibrational state, as well as the reduced mass specifying the vibrational motion, yielding thus the mass dependent Q_{int}. In the low temperature limit relevant for dark cloud conditions, the discrete rotational structure of the ground vibrational state provides the major contribution to Q_{int}. For 30 reactions $HCO^+ + CO$, given here in Table A.4 and before in Table 5 of Paper I, the factor F_q differs from 1 at most by 3.5%. Using $F_q = 1$ to compute (k_f, k_r) by means of Eq. (10), we obtain rate coefficients which differ by at most 4% from the values listed in Table A.4.

3.3. Analytic representations of the rate coefficients

For the reaction $HCO^+ + CO$, the total rate coefficients derived by Langer et al. (1984) are available for nine temperatures: 5, 10, 20, 40, 60, 80, 100, 200, and 300 K. Using these values, the forward and backward rate coefficients are determined (see Table A.4) and fit via the popular Arrhenius-Kooij formula (Kooij 1893),

$$k(T) = A \left(\frac{T}{T_{ref}} \right)^b e^{-C/T}, \qquad \text{where} \qquad T_{ref} = 298 \text{ K.} \qquad (13)$$

This analytical expansion has one nonlinear parameter, so that we employ a nonlinear least-squares technique (the Levenberg-Marquardt algorithm) to obtain optimum values for the fitting parameters (Press et al. 1985). The resulting values for A, b, and C are given in Table A.5. The statistical uncertainties are given as root-mean-square (rms) fitting errors,

$$\text{rms} = \sqrt{\frac{\sum_{i=1}^N (y_i - f_i)^2}{N}}, \qquad (14)$$

where N is the number of the known (input) data (x_i, y_i) fit by a function $f = f(x)$, so that $f_i = f(x_i)$.

The forward reaction rate coefficients k_f and the backward reaction rate coefficients k_r are fit separately since they represent elementary chemical processes. The difference between the parameters C_r for k_r and C_f for k_f is equal to the exothermicity for the corresponding isotopic exchange reaction, $C_r - C_f = \Delta E$.
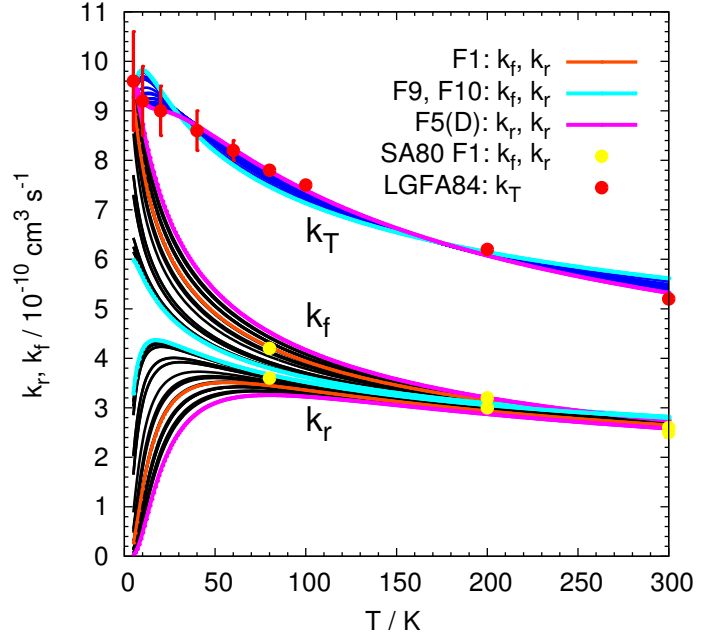
Fig. 2. Temperature dependence of the rate coefficients k_T, k_f, and k_r obtained in the fitting procedures.

This is easy to verify by comparing Tables A.3 and A.5. The fitting parameters in Table A.5 reproduce the values of the rate coefficients k_f and k_r at nine temperatures (Table A.4 of this work and Table 5 of Paper I) with rms deviations better than 2×10^{-11} cm^3 s^{-1}. Mean absolute percentage deviations are better than 4%.

The variation with temperature of the rate coefficients k_f and k_r obtained in the fitting procedures are graphically displayed in Fig. 2 for all 30 isotopic variants of the reaction $HCO^+ + CO$. At temperatures above 50 K, k_f and k_r exhibit a weak temperature dependence. The forward reaction becomes faster and the backward reaction slower as the temperature decreases, so that k_r tends to zero as $T \to 0$ K. In Fig. 2, k_f and k_r are most different for reaction F5(D), associated with the largest ΔE value of 29.4 K in Table A.3. They are least different for reactions F9 and F10, attributed the smallest ΔE value of 3.0 K (Table A.3). The experimental results of Smith & Adams (1980) available for the reaction F1 at 80, 200, and 300 K are also shown (yellow circles).

In Fig. 2, the total rate coefficients k_T (blue lines) are obtained as $k_f + k_r$ for each of the 30 reactions considered. The values of Langer et al. (1984) (red circles) are additionally shown along with their estimated uncertainties (vertical bars). Even though k_f and k_r are noticeably different for different reactions, the resulting k_T functions are similar, as expected from the model used. Our k_T results for reaction F5(D) best approximate the values of Langer et al. (1984) and can be used as an analytic representation for their values if/when needed.

The estimates of Langer et al. (1984) cover temperatures between 5 and 300 K. The analytic expressions of Table A.5 are accordingly valid only over this temperature range. Since the modified Arrhenius function of Eq. (13) goes always to zero when $T \to 0$ K, the functional representations derived for k_f will also tend to zero at temperatures below 5 K. Prior to elaborating on other forms more suitable for kinetic applications close to 0 K, one may consider the inclusion in astrochemical kinetic networks of the analytic three-parameter representations for the

rate coefficients k_f and k_r, derived here for the isotope exchange reactions HCO$^+$+CO (Table A.5).

4. Summary

In the present work, we have employed the full-dimensional quantum mechanical methods to calculate the rovibrational energies for all isotopologues of CO, HCO$^+$, and HOC$^+$ involving the isotopes H, D, ^{16}O, ^{17}O, ^{18}O, ^{12}C, and ^{13}C. These results are used to derive accurate values of the exothermicities for possible isotopic exchange reactions. For the reaction of HCO$^+$ with CO, all possible isotope fractionation variants are subsequently considered (in total 30 reactions). Values corresponding to the ^{17}O isotope are reported for the first time. The energy defects arising for the ^{17}O cases are found to be slightly smaller than those involved with ^{18}O.

For each of the reactions considered, the analytic three-parameter expressions are derived for the isotopic exchange rate coefficients k_f and k_r. These analytic representations can straightforwardly be introduced in astrochemical kinetic models in order to better understand the isotopic chemical evolution.

For all of the isotopologues of HCO$^+$ involving H, D, ^{16}O, ^{17}O, ^{18}O, ^{12}C, and ^{13}C, we provide the fundamental vibrational transitions and the rotational constants. Our best estimates of the rotational constants can provide useful assistance in analyzing expected observations of the rare forms of this cation.

References

Amano, T. 1983, J. Chem. Phys., 79, 3595
Bensch, F., Pak, I., Wouterloot, J. G. A., Klapper, G., & Winnewisser, G. 2001, ApJ, 562, L185
Davies, P. B., & Rothwell, W. J. 1984, J. Chem. Phys., 81, 5239
Dore, L., Cazzoli, G., & Caselli, P. 2001a, A&A, 368, 712
Dore, L., Puzzarini, C., & Cazzoli, G. 2001b, Can. J. Phys., 79, 359
Foster, S. C., McKeller, A. R. W., & Sears, T. J. 1984, J. Chem. Phys., 81, 578
Frerking, M. A., & Langer, W. D. 1981, J. Chem. Phys., 74, 6990
Guélin, M., Cernicharo, J., & Linke, R. A. 1982, ApJ, 263, L89
Henning, P., Kraemer, W. P., & Diercksen, G. H. F. 1977, Internal Report, MPI/PAE Astro 135, Max-Planck Institut, München
Herzberg, G. 1991, Molecular Spectra & Molecular Structure Vol. II, Infrared and Raman Spectra of Polyatomic Molecules (corrected reprint of 1945 edition) (Malabar FL: Krieger)
Hirota, E., & Endo, Y. 1988, J. Mol. Spectr., 127, 527
Kooij, D. M. 1893, Zeitschr. Phys. Chemie B, 12, 155
Langer, W. D., Graedel, T. E., Frerking, M. A., & Armentrout, P. B. 1984, ApJ, 277, 581
Li, H.-K., Zhang, J.-S., Liu, Z.-W., et al. 2016, RA&A, 16, 047
Lohr, L. L. 1998, J. Chem. Phys., 108, 8012
Mills, I., Cvitaš, T., Homann, K., Kallay, N., & Kuchitsu, K. 1993, Quantities, Units and Symbols in Physical Chemistry, 2nd edn. (Oxford: Blackwell Scientific Publications)
Mladenović, M. 2002, Spectrochim. Acta, Part A, 58, 795
Mladenović, M., & Bačić, Z. 1990, J. Chem. Phys., 93, 3039
Mladenović, M., & Roueff, E. 2014, A&A, 566, A144
Mladenović, M., & Schmatz, S. 1998, J. Chem. Phys., 109, 4456
Press, W. H., Flannery, B. P., Teukolsky, S. A., & Vetterling, W. T. 1985, Numerical Recipes, Example Book (Fortran) (Cambridge: Cambridge University Press)
Puzzarini, C., Tarroni, R., Palmieri, P., Carter, S., & Dore, L. 1996, Mol. Phys., 87, 879
Roueff, E., Loison, J. C., & Hickson, K. 2015, A&A, 576, A99
Schmatz, S., & Mladenović, M. 1997, Ber. Bunsenges. Phys. Chemie, 101, 372
Smith, D., & Adams, N. G. 1980, ApJ, 242, 424
Su, T., & Bowers, M. T. 1975, Int. J. Mass. Spec. Ion. Phys., 17, 211
Terzieva, R., & Herbst, E. 2000, MNRAS, 317, 563
Zhang, J. S., Sun, L. L., Riquelme, D., et al. 2015, ApJS, 219, 28

Appendix A: Tables

Table A.1. Computed anharmonic fundamental vibrational transitions ν_i (in cm^{-1}), estimated ground state vibrational corrections ΔB_0 (in MHz), best estimates of the rotational constant B_0^{est} (in MHz), and quartic centrifugal distortion rotational constants D_0 (in kHz) for the isotopologues of HCO$^+$.

Species	ν_1	ν_2	ν_3	ΔB_0	B_0^{est}	D_0
H^{12}C^{16}O$^+$	3085.6	830.7	2179.1	243.7	44 605.1	81.9
	[3088.7]^a	[829.7]^b	[2183.9]^c		[44 594.4]^d	[82.4]^e
H^{12}C^{17}O$^+$	3083.1	829.6	2152.3	235.4	43 539.2	78.1
					[43 528.9]^f	[79.1]^f
H^{12}C^{18}O$^+$	3081.0	828.7	2128.2	228.1	42 591.2	74.7
					[42 581.3]^d	[76]^d
H^{13}C^{16}O$^+$	3063.0	823.2	2145.4	234.1	43 387.6	77.6
					[43 377.3]^d	[79]^d
H^{13}C^{17}O$^+$	3060.9	822.1	2117.5	225.8	42 305.6	73.8
H^{13}C^{18}O$^+$	3059.1	821.2	2092.5	218.5	41 343.1	70.5
					[41 333.6]^d	[75]^d
D^{12}C^{16}O$^+$	2580.5	667.5	1900.8	173.5	36 027.6	55.2
	[2584.6]^d		[1904.1]^d		[36 019.8]^d	[55.8]^e
D^{12}C^{17}O$^+$	2566.3	666.1	1885.3	167.6	35 178.4	52.5
D^{12}C^{18}O$^+$	2554.2	665.0	2554.2	162.4	34 421.1	50.1
					[34 413.7]^g	
D^{13}C^{16}O$^+$	2529.5	658.0	1893.8	168.8	35 374.4	52.8
					[35 366.6]^g	
D^{13}C^{17}O$^+$	2515.8	656.7	1877.2	162.8	34 508.7	50.1
D^{13}C^{18}O$^+$	2504.1	655.4	1861.7	157.5	33 736.4	47.8

Notes. Experimental values are given in brackets.

References. $^{(a)}$ Amano (1983). $^{(b)}$ Davies & Rothwell (1984). $^{(c)}$ Foster et al. (1984). $^{(d)}$ Taken from Puzzarini et al. (1996). $^{(e)}$ Hirota & Endo (1988). $^{(f)}$ Dore et al. (2001b). $^{(g)}$ As given at http://physics.nist.gov/cgi-bin/MolSpec/triperiodic.pl

Table A.2. Zero point vibrational energies (in cm^{-1}) of the isotopologues of CO, HCO$^+$, and HOC$^+$.

Species	E_0	Species	E_0
^{12}C^{16}O	1079.11		
^{12}C^{17}O	1065.41		
^{12}C^{18}O	1053.11		
^{13}C^{16}O	1055.12		
^{13}C^{17}O	1041.09		
^{13}C^{18}O	1028.52		
H^{12}C^{16}O$^+$	3524.60	H^{16}O^{12}C$^+$	2871.08
H^{12}C^{17}O$^+$	3508.53	H^{17}O^{12}C$^+$	2855.41
H^{12}C^{18}O$^+$	3494.15	H^{18}O^{12}C$^+$	2841.37
H^{13}C^{16}O$^+$	3488.24	H^{16}O^{13}C$^+$	2848.66
H^{13}C^{17}O$^+$	3471.85	H^{17}O^{13}C$^+$	2832.71
H^{13}C^{18}O$^+$	3457.16	H^{18}O^{13}C$^+$	2818.42
D^{12}C^{16}O$^+$	2946.08	D^{16}O^{12}C$^+$	2357.61
D^{12}C^{17}O$^+$	2929.54	D^{17}O^{12}C$^+$	2340.97
D^{12}C^{18}O$^+$	2914.72	D^{18}O^{12}C$^+$	2326.06
D^{13}C^{16}O$^+$	2907.02	D^{16}O^{13}C$^+$	2334.87
D^{13}C^{17}O$^+$	2890.15	D^{17}O^{13}C$^+$	2317.97
D^{13}C^{18}O$^+$	2875.03	D^{18}O^{13}C$^+$	2302.82

Table A.3. Zero point energy differences ΔE between the reactants and products for the isotope fractionation reactions of H/DCO$^+$ and H/DOC$^+$ with CO.

Label	Reaction	ΔE/K	Label	Reaction	ΔE/K
	^{13}C$^+$+^{12}C^{16}O → ^{12}C$^+$+^{13}C^{16}O	34.5			
	^{13}C$^+$+^{12}C^{17}O → ^{12}C$^+$+^{13}C^{17}O	35.0			
	^{13}C$^+$+^{12}C^{18}O → ^{12}C$^+$+^{13}C^{18}O	35.4			
F1	H^{12}C^{16}O$^+$+^{13}C^{16}O → H^{13}C^{16}O$^+$+^{12}C^{16}O	17.8	I1	H^{16}O^{12}C$^+$+^{13}C^{16}O → H^{16}O^{13}C$^+$+^{12}C^{16}O	−2.3
F2	H^{12}C^{18}O$^+$+^{13}C^{18}O → H^{13}C^{18}O$^+$+^{12}C^{18}O	17.8	I2	H^{18}O^{12}C$^+$+^{13}C^{18}O → H^{18}O^{13}C$^+$+^{12}C^{18}O	−2.4
F3	H^{12}C^{16}O$^+$+^{12}C^{18}O → H^{12}C^{18}O$^+$+^{12}C^{16}O	6.4	I3	H^{16}O^{12}C$^+$+^{12}C^{18}O → H^{18}O^{12}C$^+$+^{12}C^{16}O	5.3
F4	H^{13}C^{16}O$^+$+^{13}C^{18}O → H^{13}C^{18}O$^+$+^{13}C^{16}O	6.4	I4	H^{16}O^{13}C$^+$+^{13}C^{18}O → H^{18}O^{13}C$^+$+^{13}C^{16}O	5.2
F5	H^{12}C^{16}O$^+$+^{13}C^{18}O → H^{13}C^{18}O$^+$+^{12}C^{16}O	24.2	I5	H^{16}O^{12}C$^+$+^{13}C^{18}O → H^{18}O^{13}C$^+$+^{12}C^{16}O	3.0
F6	H^{12}C^{18}O$^+$+^{13}C^{16}O → H^{13}C^{16}O$^+$+^{12}C^{18}O	11.4	I6	H^{18}O^{12}C$^+$+^{13}C^{16}O → H^{16}O^{13}C$^+$+^{12}C^{18}O	−7.6
F7	H^{12}C^{16}O$^+$+^{12}C^{17}O → H^{12}C^{17}O$^+$+^{12}C^{16}O	3.4	I7	H^{16}O^{12}C$^+$+^{12}C^{17}O → H^{17}O^{12}C$^+$+^{12}C^{16}O	2.8
F8	H^{13}C^{16}O$^+$+^{13}C^{17}O → H^{13}C^{17}O$^+$+^{13}C^{16}O	3.4	I8	H^{16}O^{13}C$^+$+^{13}C^{17}O → H^{17}O^{13}C$^+$+^{13}C^{16}O	2.8
F9	H^{12}C^{17}O$^+$+^{12}C^{18}O → H^{12}C^{18}O$^+$+^{12}C^{17}O	3.0	I9	H^{17}O^{12}C$^+$+^{12}C^{18}O → H^{18}O^{12}C$^+$+^{12}C^{17}O	2.5
F10	H^{13}C^{17}O$^+$+^{13}C^{18}O → H^{13}C^{18}O$^+$+^{13}C^{17}O	3.0	I10	H^{17}O^{13}C$^+$+^{13}C^{18}O → H^{18}O^{13}C$^+$+^{13}C^{17}O	2.5
F11	H^{12}C^{16}O$^+$+^{13}C^{17}O → H^{13}C^{17}O$^+$+^{12}C^{16}O	21.2	I11	H^{16}O^{12}C$^+$+^{13}C^{17}O → H^{17}O^{13}C$^+$+^{12}C^{16}O	0.5
F12	H^{12}C^{17}O$^+$+^{13}C^{17}O → H^{13}C^{17}O$^+$+^{12}C^{17}O	17.8	I12	H^{17}O^{12}C$^+$+^{13}C^{17}O → H^{17}O^{13}C$^+$+^{12}C^{17}O	−2.3
F13	H^{12}C^{18}O$^+$+^{13}C^{17}O → H^{13}C^{17}O$^+$+^{12}C^{18}O	14.8	I13	H^{18}O^{12}C$^+$+^{13}C^{17}O → H^{17}O^{13}C$^+$+^{12}C^{18}O	−4.8
F14	H^{12}C^{17}O$^+$+^{13}C^{16}O → H^{13}C^{16}O$^+$+^{12}C^{17}O	14.4	I14	H^{17}O^{12}C$^+$+^{13}C^{16}O → H^{16}O^{13}C$^+$+^{12}C^{17}O	−5.1
F15	H^{12}C^{17}O$^+$+^{13}C^{18}O → H^{13}C^{18}O$^+$+^{12}C^{17}O	20.8	I15	H^{17}O^{12}C$^+$+^{13}C^{18}O → H^{18}O^{13}C$^+$+^{12}C^{17}O	0.1
F1(D)	D^{12}C^{16}O$^+$+^{13}C^{16}O → D^{13}C^{16}O$^+$+^{12}C^{16}O	21.7	I1(D)	D^{16}O^{12}C$^+$+^{13}C^{16}O → D^{16}O^{13}C$^+$+^{12}C^{16}O	−1.8
F2(D)	D^{12}C^{18}O$^+$+^{13}C^{18}O → D^{13}C^{18}O$^+$+^{12}C^{18}O	21.7	I2(D)	D^{18}O^{12}C$^+$+^{13}C^{18}O → D^{18}O^{13}C$^+$+^{12}C^{18}O	−1.9
F3(D)	D^{12}C^{16}O$^+$+^{12}C^{18}O → D^{12}C^{18}O$^+$+^{12}C^{16}O	7.7	I3(D)	D^{16}O^{12}C$^+$+^{12}C^{18}O → D^{18}O^{12}C$^+$+^{12}C^{16}O	8.0
F4(D)	D^{13}C^{16}O$^+$+^{13}C^{18}O → D^{13}C^{18}O$^+$+^{13}C^{16}O	7.7	I4(D)	D^{16}O^{13}C$^+$+^{13}C^{18}O → D^{18}O^{13}C$^+$+^{13}C^{16}O	7.8
F5(D)	D^{12}C^{16}O$^+$+^{13}C^{18}O → D^{13}C^{18}O$^+$+^{12}C^{16}O	29.4	I5(D)	D^{16}O^{12}C$^+$+^{13}C^{18}O → D^{18}O^{13}C$^+$+^{12}C^{16}O	6.0
F6(D)	D^{12}C^{18}O$^+$+^{13}C^{16}O → D^{13}C^{16}O$^+$+^{12}C^{18}O	14.0	I6(D)	D^{18}O^{12}C$^+$+^{13}C^{16}O → D^{16}O^{13}C$^+$+^{12}C^{18}O	−9.8
F7(D)	D^{12}C^{16}O$^+$+^{12}C^{17}O → D^{12}C^{17}O$^+$+^{12}C^{16}O	4.1	I7(D)	D^{16}O^{12}C$^+$+^{12}C^{17}O → D^{17}O^{12}C$^+$+^{12}C^{16}O	4.2
F8(D)	D^{13}C^{16}O$^+$+^{13}C^{17}O → D^{13}C^{17}O$^+$+^{13}C^{16}O	4.1	I8(D)	D^{16}O^{13}C$^+$+^{13}C^{17}O → D^{17}O^{13}C$^+$+^{13}C^{16}O	4.1
F9(D)	D^{12}C^{17}O$^+$+^{12}C^{18}O → D^{12}C^{18}O$^+$+^{12}C^{17}O	3.6	I9(D)	D^{17}O^{12}C$^+$+^{12}C^{18}O → D^{18}O^{12}C$^+$+^{12}C^{17}O	3.8
F10(D)	D^{13}C^{17}O$^+$+^{13}C^{18}O → D^{13}C^{18}O$^+$+^{13}C^{17}O	3.7	I10(D)	D^{17}O^{13}C$^+$+^{13}C^{18}O → D^{18}O^{13}C$^+$+^{13}C^{17}O	3.7
F11(D)	D^{12}C^{16}O$^+$+^{13}C^{17}O → D^{13}C^{17}O$^+$+^{12}C^{16}O	25.8	I11(D)	D^{16}O^{12}C$^+$+^{13}C^{17}O → D^{17}O^{13}C$^+$+^{12}C^{16}O	2.3
F12(D)	D^{12}C^{17}O$^+$+^{13}C^{17}O → D^{13}C^{17}O$^+$+^{12}C^{17}O	21.7	I12(D)	D^{17}O^{12}C$^+$+^{13}C^{17}O → D^{17}O^{13}C$^+$+^{12}C^{17}O	−1.9
F13(D)	D^{12}C^{18}O$^+$+^{13}C^{17}O → D^{13}C^{17}O$^+$+^{12}C^{18}O	18.1	I13(D)	D^{18}O^{12}C$^+$+^{13}C^{17}O → D^{17}O^{13}C$^+$+^{12}C^{18}O	−5.7
F14(D)	D^{12}C^{17}O$^+$+^{13}C^{16}O → D^{13}C^{16}O$^+$+^{12}C^{17}O	17.6	I14(D)	D^{17}O^{12}C$^+$+^{13}C^{16}O → D^{16}O^{13}C$^+$+^{12}C^{17}O	−6.0
F15(D)	D^{12}C^{17}O$^+$+^{13}C^{18}O → D^{13}C^{18}O$^+$+^{12}C^{17}O	25.3	I15(D)	D^{17}O^{12}C$^+$+^{13}C^{18}O → D^{18}O^{13}C$^+$+^{12}C^{17}O	1.8

Table A.4. Equilibrium constants K_e, partition function factors F_q, and rate coefficients k_f, k_r (in 10^{-10} cm^3 s^{-1}) for the reactions of H/DCO$^+$ with CO involving the isotope ^{17}O.

Reaction	T/K	5	10	20	40	60	80	100	200	300
F7	F_q	0.9981	0.9974	0.9971	0.9970	0.9969	0.9969	0.9969	0.9969	0.9970
	K_e	1.97	1.40	1.18	1.09	1.05	1.04	1.03	1.01	1.01
	(k_f, k_r)	(6.36, 3.24)	(5.37, 3.83)	(4.87, 4.13)	(4.48, 4.12)	(4.21, 3.99)	(3.98, 3.82)	(3.81, 3.69)	(3.12, 3.08)	(2.61, 2.59)
F8	F_q	0.9981	0.9974	0.9971	0.9969	0.9969	0.9969	0.9969	0.9969	0.9970
	K_e	1.97	1.40	1.18	1.09	1.06	1.04	1.03	1.01	1.01
	(k_f, k_r)	(6.37, 3.23)	(5.37, 3.83)	(4.88, 4.12)	(4.48, 4.12)	(4.21, 3.99)	(3.98, 3.82)	(3.81, 3.69)	(3.12, 3.08)	(2.61, 2.59)
F9	F_q	0.9983	0.9977	0.9974	0.9973	0.9972	0.9972	0.9972	0.9972	0.9973
	K_e	1.82	1.35	1.16	1.08	1.05	1.04	1.03	1.01	1.01
	(k_f, k_r)	(6.20, 3.40)	(5.28, 3.92)	(4.83, 4.17)	(4.46, 4.14)	(4.20, 4.00)	(3.97, 3.83)	(3.80, 3.70)	(3.12, 3.08)	(2.61, 2.59)
F10	F_q	0.9982	0.9977	0.9974	0.9973	0.9972	0.9972	0.9972	0.9972	0.9973
	K_e	1.83	1.35	1.16	1.08	1.05	1.04	1.03	1.01	1.01
	(k_f, k_r)	(6.21, 3.39)	(5.29, 3.91)	(4.84, 4.16)	(4.46, 4.14)	(4.20, 4.00)	(3.97, 3.83)	(3.80, 3.70)	(3.12, 3.08)	(2.61, 2.59)
F11	F_q	0.9835	0.9806	0.9793	0.9786	0.9784	0.9783	0.9782	0.9784	0.9795
	K_e	68.17	8.16	2.83	1.66	1.39	1.27	1.21	1.09	1.05
	(k_f, k_r)	(9.46, 0.14)	(8.20, 1.00)	(6.65, 2.35)	(5.37, 3.23)	(4.77, 3.43)	(4.37, 3.43)	(4.10, 3.40)	(3.23, 2.97)	(2.66, 2.54)
F12	F_q	0.9854	0.9832	0.9821	0.9816	0.9814	0.9813	0.9813	0.9815	0.9824
	K_e	34.67	5.83	2.39	1.53	1.32	1.23	1.17	1.07	1.04
	(k_f, k_r)	(9.33, 0.27)	(7.85, 1.35)	(6.35, 2.65)	(5.20, 3.40)	(4.67, 3.53)	(4.30, 3.50)	(4.05, 3.45)	(3.21, 2.99)	(2.65, 2.55)
F13	F_q	0.9870	0.9854	0.9847	0.9843	0.9841	0.9841	0.9840	0.9842	0.9851
	K_e	19.03	4.33	2.06	1.42	1.26	1.18	1.14	1.06	1.03
	(k_f, k_r)	(9.12, 0.48)	(7.47, 1.73)	(6.06, 2.94)	(5.05, 3.55)	(4.57, 3.63)	(4.23, 3.57)	(4.00, 3.50)	(3.19, 3.01)	(2.64, 2.56)
F14	F_q	0.9873	0.9857	0.9850	0.9846	0.9845	0.9844	0.9844	0.9845	0.9854
	K_e	17.57	4.16	2.02	1.41	1.25	1.18	1.14	1.06	1.03
	(k_f, k_r)	(9.08, 0.52)	(7.42, 1.78)	(6.02, 2.98)	(5.03, 3.57)	(4.56, 3.64)	(4.22, 3.58)	(3.99, 3.51)	(3.19, 3.01)	(2.64, 2.56)
F15	F_q	0.9836	0.9809	0.9795	0.9789	0.9787	0.9786	0.9785	0.9787	0.9798
	K_e	63.58	7.89	2.78	1.65	1.39	1.27	1.21	1.09	1.05
	(k_f, k_r)	(9.45, 0.15)	(8.16, 1.04)	(6.62, 2.38)	(5.35, 3.25)	(4.76, 3.44)	(4.36, 3.44)	(4.10, 3.40)	(3.23, 2.97)	(2.66, 2.54)
F7(D)	F_q	0.9969	0.9958	0.9953	0.9950	0.9950	0.9949	0.9949	0.9950	0.9953
	K_e	2.25	1.50	1.22	1.10	1.06	1.05	1.04	1.02	1.01
	(k_f, k_r)	(6.65, 2.95)	(5.52, 3.68)	(4.95, 4.05)	(4.51, 4.09)	(4.23, 3.97)	(3.99, 3.81)	(3.82, 3.68)	(3.12, 3.08)	(2.61, 2.59)
F8(D)	F_q	0.9968	0.9957	0.9952	0.9950	0.9949	0.9949	0.9948	0.9950	0.9953
	K_e	2.26	1.50	1.22	1.10	1.07	1.05	1.04	1.02	1.01
	(k_f, k_r)	(6.65, 2.95)	(5.52, 3.68)	(4.95, 4.05)	(4.51, 4.09)	(4.23, 3.97)	(3.99, 3.81)	(3.82, 3.68)	(3.12, 3.08)	(2.61, 2.59)
F9(D)	F_q	0.9971	0.9962	0.9957	0.9955	0.9955	0.9954	0.9954	0.9955	0.9958
	K_e	2.06	1.43	1.19	1.09	1.06	1.04	1.03	1.01	1.01
	(k_f, k_r)	(6.46, 3.14)	(5.42, 3.78)	(4.90, 4.10)	(4.49, 4.11)	(4.21, 3.99)	(3.98, 3.82)	(3.81, 3.69)	(3.12, 3.08)	(2.61, 2.59)
F10(D)	F_q	0.9970	0.9961	0.9957	0.9955	0.9954	0.9954	0.9954	0.9955	0.9958
	K_e	2.07	1.44	1.20	1.09	1.06	1.04	1.03	1.01	1.01
	(k_f, k_r)	(6.48, 3.12)	(5.42, 3.78)	(4.90, 4.10)	(4.49, 4.11)	(4.22, 3.98)	(3.98, 3.82)	(3.81, 3.69)	(3.12, 3.08)	(2.61, 2.59)
F11(D)	F_q	0.9733	0.9691	0.9671	0.9661	0.9658	0.9657	0.9656	0.9667	0.9692
	K_e	168.50	12.75	3.51	1.84	1.48	1.33	1.25	1.10	1.06
	(k_f, k_r)	(9.54, 0.06)	(8.53, 0.67)	(7.00, 2.00)	(5.57, 3.03)	(4.90, 3.30)	(4.46, 3.34)	(4.17, 3.33)	(3.25, 2.95)	(2.67, 2.53)
F12(D)	F_q	0.9763	0.9732	0.9717	0.9710	0.9707	0.9706	0.9706	0.9715	0.9738
	K_e	74.76	8.52	2.87	1.67	1.39	1.27	1.21	1.08	1.05
	(k_f, k_r)	(9.47, 0.13)	(8.23, 0.97)	(6.68, 2.32)	(5.38, 3.22)	(4.77, 3.43)	(4.37, 3.43)	(4.10, 3.40)	(3.22, 2.98)	(2.66, 2.54)
F13(D)	F_q	0.9791	0.9769	0.9759	0.9753	0.9752	0.9751	0.9750	0.9759	0.9779
	K_e	36.27	5.95	2.41	1.53	1.32	1.22	1.17	1.07	1.04
	(k_f, k_r)	(9.34, 0.26)	(7.88, 1.32)	(6.36, 2.64)	(5.20, 3.40)	(4.66, 3.54)	(4.29, 3.51)	(4.04, 3.46)	(3.20, 3.00)	(2.65, 2.55)
F14(D)	F_q	0.9795	0.9774	0.9764	0.9759	0.9757	0.9756	0.9756	0.9764	0.9784
	K_e	33.10	5.68	2.35	1.52	1.31	1.22	1.16	1.07	1.04
	(k_f, k_r)	(9.32, 0.28)	(7.82, 1.38)	(6.32, 2.68)	(5.18, 3.42)	(4.65, 3.55)	(4.28, 3.52)	(4.03, 3.47)	(3.20, 3.00)	(2.65, 2.55)
F15(D)	F_q	0.9734	0.9694	0.9675	0.9666	0.9663	0.9661	0.9661	0.9671	0.9697
	K_e	154.91	12.23	3.44	1.82	1.47	1.33	1.24	1.10	1.06
	(k_f, k_r)	(9.54, 0.06)	(8.50, 0.70)	(6.97, 2.03)	(5.55, 3.05)	(4.89, 3.31)	(4.45, 3.35)	(4.16, 3.34)	(3.24, 2.96)	(2.67, 2.53)

Table A.5. Fitting parameters A (in 10^{-10} cm^3 s^{-1}), b, and C (in K) for the forward rate coefficients k_f and the reverse rate coefficients k_r for the reactions of HCO$^+$ with CO.

Reaction	k_f				k_r			
	A_f	b_f	C_f	rms	A_r	b_r	C_r	rms
F1	2.77	−0.33	0.64	0.08	2.82	−0.33	18.46	0.06
F2	2.77	−0.33	0.65	0.08	2.82	−0.33	18.51	0.06
F3	2.82	−0.25	0.32	0.19	2.83	−0.25	6.73	0.13
F4	2.82	−0.25	0.32	0.19	2.83	−0.25	6.78	0.13
F5	2.77	−0.37	1.31	0.06	2.84	−0.37	25.59	0.04
F6	2.79	−0.28	0.16	0.14	2.83	−0.28	11.56	0.09
F7	2.83	−0.23	0.91	0.20	2.84	−0.23	4.31	0.16
F8	2.83	−0.23	0.91	0.20	2.84	−0.23	4.32	0.16
F9	2.83	−0.23	1.02	0.20	2.84	−0.23	4.04	0.17
F10	2.83	−0.23	1.01	0.20	2.84	−0.23	4.06	0.17
F11	2.77	−0.35	0.99	0.07	2.83	−0.35	22.22	0.05
F12	2.77	−0.33	0.65	0.08	2.82	−0.33	18.48	0.06
F13	2.78	−0.31	0.37	0.10	2.82	−0.31	15.19	0.07
F14	2.78	−0.30	0.34	0.11	2.82	−0.30	14.75	0.07
F15	2.77	−0.35	0.96	0.07	2.83	−0.35	21.84	0.05
F1(D)	2.76	−0.35	1.03	0.06	2.84	−0.35	22.76	0.05
F2(D)	2.76	−0.35	1.03	0.06	2.84	−0.35	22.80	0.05
F3(D)	2.81	−0.26	0.19	0.18	2.83	−0.26	7.93	0.12
F4(D)	2.81	−0.26	0.19	0.17	2.83	−0.26	7.96	0.12
F5(D)	2.77	−0.39	1.80	0.04	2.87	−0.39	31.30	0.03
F6(D)	2.78	−0.30	0.29	0.11	2.83	−0.30	14.29	0.08
F7(D)	2.83	−0.24	0.73	0.20	2.84	−0.24	4.82	0.16
F8(D)	2.83	−0.24	0.73	0.20	2.84	−0.24	4.83	0.16
F9(D)	2.83	−0.24	0.84	0.20	2.84	−0.24	4.49	0.16
F10(D)	2.83	−0.24	0.84	0.20	2.84	−0.24	4.51	0.16
F11(D)	2.76	−0.37	1.45	0.05	2.85	−0.38	27.28	0.04
F12(D)	2.76	−0.35	1.03	0.06	2.84	−0.35	22.77	0.05
F13(D)	2.76	−0.33	0.66	0.08	2.83	−0.33	18.76	0.06
F14(D)	2.77	−0.33	0.61	0.08	2.83	−0.33	18.25	0.06
F15(D)	2.76	−0.37	1.41	0.05	2.85	−0.37	26.82	0.04

Notes. The rms fitting errors (in 10^{-10} cm^3 s^{-1}) are calculated using Eq. (14).